Aiding Classical-Quantum Protocol Stack with Classical Error Correction: An IoT Perspective

Siddharth Das ‡†, Riccardo Bassoli ‡†*, and Frank H. P. Fitzek ‡*
‡ Deutsche Telekom Chair of Communication Networks, Technische Universität Dresden, Dresden, Germany.
† Quantum Communication Networks (QCNets) research group, Technische Universität Dresden, Dresden, Germany.
∗ Centre for Tactile Internet with Human-in-the-Loop (CeTI), Cluster of Excellence, Dresden, Germany.
Emails: {siddharth.das, riccardo.bassoli, frank.fitzek}@tu-dresden.de

2024 IEEE 10th World Forum on Internet of Things (WF-IoT) | 979-8-3503-7301-1/24/$31.00 ©2024 IEEE | DOI: 10.1109/WF-IoT62078.2024.10811366

***Abstract*—In the context of integrating quantum principles into the Internet of Things (IoT) network to enhance capacity, security, and resilience, we present a classical-quantum (CQ) protocol stack that can be systematically integrated into a classical network. The CQ architecture explicitly defines the physical and link layer behavior to accommodate quantum functionalities. We demonstrate how the use of classical error correction codes (ECC) is practical within a quantum communication protocol integrated into a classical network setup. Furthermore, we have modeled a method to calculate the classical capacity of quantum-assisted transmission over a noisy quantum channel that employs classical ECC. As a proof of concept, we have emulated classical packet transmission through various layers of the proposed protocol stack, and the behavior has been analyzed.**

***Index Terms*—Entanglement-assisted communication, quantum network simulation, classical network emulation.**

I. Introduction

A generational development from first to fifth generation of communication network have proliferated advances in internet of things (IoT) technology. More and more devices are interconnected to provide ubiquitous sensing and computing capabilities. It is predicted that by 2030, almost 500 billion devices are expected to be connected to the Internet [1]. Although 5G has improved the quality of service in comparison to earlier generation, it will be incapacitated by the requirements posed by completely automated and intelligent network after 10 years [2]. The step towards 6G focuses on the convergence of communication, intelligence, sensing, control, and computing communication; which was neglected by 5G [3]. With the growing interconnected devices, it is predicted that the net traffic will grow exponentially over 5000 ExaByte (EB) in 2030 [4]. Additionally, application of machine learning in IoT for high multi-dimensional data classification will encounter processing deficiency and transmission overhead [5]. For compensating the exponentially growing datasets, data processing and computational efficiency has to be enhanced. However, Moore's law [6] has experienced a decline in semiconductor development urging other alternatives to fulfil the demands posed. Under the umbrella of 6G, quantum technologies are being considered in bolstering IoT by providing inherent parallelism, security, and higher data rates by exploiting fundamental properties of quantum mechanics. Several proposed quantum-aided solutions in multi-objective routing and load balancing, channel estimations, decoding, localization, and multi-user transmission has already been proposed in [7], [8], and [9], which assists a wireless-based network.

Within the scope of this article, we attempted to present a classical-quantum (CQ) protocol stack which can enable the integration of quantum technologies in IoT-based network. Considering the importance of security and data transmission in an IoT network, we have studied the transmission of classical information by quantum-assisted communication protocols between two nodes. We have implemented a practical scenario where data propagates via simulated noisy quantum channel. In a CQ architecture, both classical and quantum error correction code (ECC) can be used. However, quantum error correction (QEC) uses ancillary quantum bits or qubits to create higher-dimensional code space which has experimental and practical limitations in terms of computation. Taking into account the resource-limited aspect of IoT-based devices, we propose the usage of classical ECC for carrying out a quantum-assisted communication protocol which is lightweight and easily integrable. Further on, we also describe how the proposed methods changes the protocol stack to accommodate quantum abilities. We have also developed mathematical means to analyze the capacity of quantum-assisted protocol in a noisy scenario. For demonstration of our proposed methods, we have transmitted an image file between two communicating nodes.

The rest of the paper is organised as follows. Section II describes the system model and implemented protocol stack describing physical and link layer. Section III outlines the simulation setup and associated configurations. We report our findings and results in Section IV. Ultimately, Section V concludes our work with a brief discussion and future direction.

II. System Model

In this section we materialize the system model of the emulation. The system model has been implemented in a platform termed as "Qontainernet", which integrates quantum network simulation provided by quantum network simulator (QuNetSim) inside a classical network emulator communication network emulator (ComNetsEmu) as presented in [10].

Several protocol stack model specifically in the case of quantum communication have been provided in various literature [11], [12]. A quantum protocol stack commonly found in most literature consists of: a physical layer, link layer, and a network layer. The definition of the architectural characteristics of the protocol stack (in mentioned literature, specifically) takes in account of certain assumptions which are aligned with current technology and are open for future modifications as per the research intensifies. The current work focuses majorly on the implementation and functionality of the physical and link layer.

A. Physical Layer Characteristics

In the literature [12] and [11] concerning quantum stack model, the authors have described the physical layer as a medium for qubit transmission. In [11], physical layer has an added responsibility of being a facilitator to switch between different quantum technologies as required by the application. This means, in a quantum network if a qubit needs to be stored then it can be stored in an ion-trap or NV-center. At the same time, if a qubit is to be transmitted, then the node can choose an optical setup for said transmission. However, within the scope of this work, the physical layer is only considered as a medium for qubit transmission with a suitable error model for the simplicity of the simulation-emulation. QuNetSim does not have an explicit definition of physical layer. Additionally, Qontainernet considers an error-free transmission of qubits over the quantum channel. In this work, instead of an ideal scenario we have introduced quantum depolarizing channel as a quantum decoherence model at the physical layer. The choice of noise is merely for demonstration purpose, any noise model can be chosen instead.

The depolarizing noise can be modelled as a completely trace preserving linear map $\mathcal{E}$ acting on a quantum state ρ as following

$$\mathcal{E}(\rho) = \sum_{i=0}^{3} p_i \mathcal{K}_i \rho \mathcal{K}_i^{\dagger}, \tag{1}$$

where, $\mathcal{K}$ is the Kraus operator signifying the Pauli matrices (X, Y, and Z gates respectively) and p is the probability. Since classical information is encoded into quantum states, the classical capacity of quantum depolarizing noise is an essential factor that needs to be considered. The classical capacity of quantum depolarizing noise has been derived in great detail in [13]. The author has compared the quanutm depolarizing channel to a classical binary symmetric channel (BSC). The prior entanglement generation is noiseless in QuNetSim which can be mapped to a one-sided channel [13]. The entanglement-assisted communication protocol of superdense coding has been implemented and therefore, the channel capacity was observed accordingly. In an ideal scenario considering the analogy of Alice and Bob, the superdense coding capacity for unitary encoding, can be written as

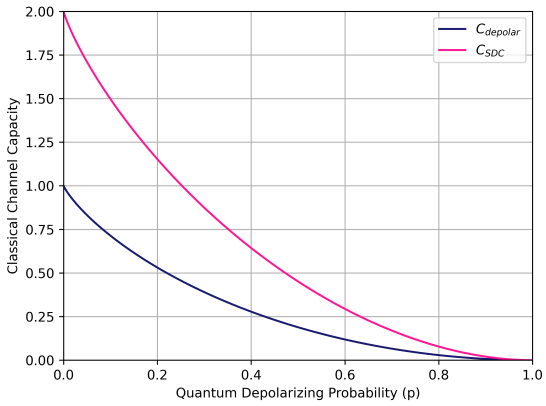

Fig. 1. Classical capacities of superdense coding and depolarizing channel against increasing depolarizing probability p.

$$C = 1 + S(\rho_b) - S(\rho). \tag{2}$$

Where, ρ is the initial bipartite state shared between Alice and Bob. ρ_b is Bob's reduced density operator and $S(.)$ is the von Neumann entropy. If quantum noise come to effect, the capacity C in (2) reflects the detrimental effects and can be represented as [13]

$$C_{depolar} = 1 + \frac{2-p}{2}\log\frac{2-p}{2} + \frac{p}{2}\log_2\frac{p}{2}. \tag{3}$$

Where, p signifies the quantum depolarizing noise parameter. Similarly, the entanglement-assisted channel capacity of superdense coding has been derived based on the equivalence to classical $M-$array symmetric discrete channel [13]

$$C_{SDC} = 2 + \frac{4-3p}{4}\log_2\frac{4-3p}{4} + 3\frac{p}{4}\log_2\frac{p}{4}. \tag{4}$$

Fig. 1 depicts the classical capacity of quantum depolarizing channel $C_{depolar}$ and entanglement-assisted superdense coding capacity C_{SDC} as a function of increasing depolarizing noise p. It can be seen from Fig. 1, in ideal case, superdense coding results in maximum transmission of classical information in comparison to scenario concerning $C_{depolar}$.

B. Link Layer Characteristics

In the quantum network stack presented in [12], the link layer is responsible for establishing robust multi-party entanglement between various network nodes. The robustness is created by multiple attempts to establish entanglement until success when a request for entanglement generation has been raised. Whereas, Pirker and Dür [11] presented a novel "connectivity layer" that has no correspondence in the Open System Interconnect (OSI) model [14]. The connectivity layer instead provides the mechanism to tackle errors encountered

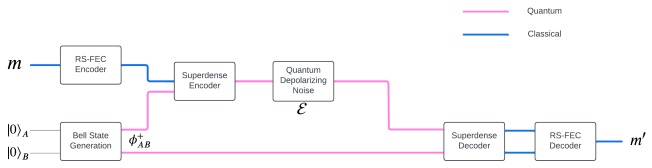

Fig. 2. System model depicting superdense coding protocol combined with RS forward error correction.

due to the imperfections of the quantum channel pertaining to physical layer. Techniques for establishing long-distance entanglement is encapsulated by the connectivity layer with the assistance of technologies such as quantum repeaters [15] or percolation/distillation techniques. Additionally, the link layer also defines the topological aspects of the network in terms of the shared entanglement between nodes.

In this article, the link layer is responsible for encoding the classical information using a classical error correction scheme which then maps it onto a suitable quantum state for its transmission through the physical layer. If an entanglement-assisted communication protocol is chosen, then network nodes store and distribute Einstein Podolsky Rosen (EPR) pairs to facilitate the protocol. However, if the network does not use any entanglement-assisted protocol, then one bit is encoded as one qubit. In the context of reliability, classical packet transmission relies on packet re-transmission in case of error or packet drops. In the quantum domain because of no-cloning theorem, copies of packet can not be stored for re-transmission. Though, a form of re-transmission has been proposed in [16] that can be employed between entangled states using secret-key sharing [17]. By minimizing packet re-transmission, the channel can be much efficiently used. With that perspective, inclusion of forward error correction (FEC) schemes are beneficial. In our previous work [18], and in another separate work [19], we observed the coding efficiency of classical error correction schemes in comparison to QEC schemes.

C. System Model Encapsulating Physical and Link Layer

The physical and link layer characteristics presented in Section II-A and Section II-B, respectively, gives way to the system model depicted in Fig. 2. The entanglement-assisted protocol of superdense coding is the primary mode of communication for the transmission of classical information in our work.

Fig. 2 briefly describes the CQ circuital model proposed in our work. A superdense coding protocol has been depicted with a feed through of classically encoded message to the superdense encoder which transmits quantum states via a quantum depolarizing channel $\mathcal{E}$. The blue lines indicate a classical link, whereas the pink lines are pure quantum links. The communicating nodes — in this analogy, Alice and Bob, share an entangled state prior to the communication. The entangled or Bell-state shared by Alice and Bob is $\left|\phi^+_{AB}\right\rangle = \frac{1}{\sqrt{2}}(|00\rangle + |11\rangle)$. Initially, the classical message m of length k bits, that is to be sent is first encoded by a RS encoder, which forms an n bit codeword. The encoding enlarges the message by a n/k factor. For example, if n is the codeword then $n = Gm$ where, G is the generator matrix. The length of codeword is dependent upon the type of (n, k) RS coding. The encoded binary message is then pair-wise assembled and fed to the superdense encoder as displayed in Fig. 2. The superdense encoder encodes the $2-$bit classical message to corresponding Bell states $|\phi^+\rangle, |\phi^-\rangle, |\psi^+\rangle$, and, $|\psi^-\rangle$. To avoid additional padding, the codeword has been considered of $2n$ bits. A generalised equation for the net ensemble ρ_m of state sent from Alice to Bob can be simply formulated as

$$\rho_m = \prod_{i=0}^{n-1} U_A(c_{2i}, c_{2i+1})\rho_0 U_A(c_{2i}, c_{2i+1})^\dagger. \tag{5}$$

Here, c_i is the i-th bit, U_A denotes the unitary encoding of binary bits from Alice's side, i.e. $U_A(m_o, m_1) = X_A^{m_0} Z_A^{m_1}$. At Bob's end, message m' is received which has the detrimental effects of the introduced channel noise. The received message by Bob can be written in terms of transition probability as following:

$$P(m'|m) = Tr\left[\prod_{m'} \mathcal{E}(\rho_b)\right]. \tag{6}$$

$\prod_{m'}$ is the projection operator of the complete set of Bell measurements, $\mathcal{E}(\rho_b)$ is the application of depolarizing noise on the density matrix of the sent message, and $Tr[.]$ is the trace of the matrix. Once Bob measures the quantum states, he is left with the classical message with potential errors introduced by the depolarizing channel. The physical and link layer protocols thus presented in the Fig. 2 incorporates the network layers which were missing from QuNetSim network architecture. Various layers of the stack model along with the incorporated physical and link layer for QuNetSim is depicted in Fig. 3.

III. Simulation Setup

Fig. 4 describes the outlook of the entire simulation and the flow of data. It depicts the integrated link and physical layer, provided by QuNetSim, in ComNetsEmu. Various docker containers, namely, Alice and Bob container, and quantum bridge container is depicted in Fig. 4. Hosts Alice and Bob have specific internet protocol (IP) addresses signifying a point-to-point source and destination link. The quantum bridge container acts as a relay between the communicating hosts, that has the quantum notion inside. Data generated at Alice's container is first encoded with RS code and then an IP packet is formed which is routed to the bridge container. Qontainernet has two types of frames — data frames and EPR frames. The data frame carries the classical message, whereas the EPR

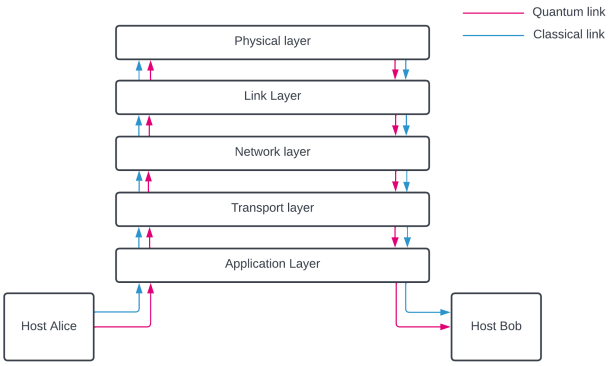

Fig. 3. Architecture of QuNetSim after the implementation of physical and link layer.

frame has collection of EPR pairs. The quantum bridge container — a dockerized instance of QuNetSim, decomposes the IP packets into bits which are then mapped to quantum states for the transmission over the quantum channel inside the same container. After mapping classical bits into qubits, the header qubit is used to decide whether a packet is either data frame or an EPR frame. This way, QuNetSim hosts decide whether to send a qubit or to share an EPR with other QuNetSim host. Afterwards, the quantum states travel from one QuNetSim host A to the other B in the quantum bridge container. The quantum channel is modelled with depolarizing noise as mentioned in the II-A. Once QuNetSim host B receives and decodes the quantum frame, IP packet is reconstructed and routed to Host Bob container. The data transmission for the current study, has been in the form of bursts, which is common in sensor technology and IoT. Idle periods in between bursts are filled with entanglement distribution between Alice and Bob demonstrating the "generate entanglement when idle" principle [20]. The amount of entanglement shared between two parties is a simulation parameter and can be tuned pertaining to the application.

IV. Results and Discussion

In this section we will address our finding regarding the simulation-emulation carried out in Qontainernet. The evaluation of simulation-emulation have been reported in Section IV-A and Section IV-B. Finally, in Section IV-C we demonstrate an application of transmitting an image file.

A. Bit Error Rate Analysis

The performance of RS code has been analysed in terms of bit error rate (BER). All the packets were transmitted in bursts using the entanglement-assisted protocol of superdense coding. The idle periods in between bursts were allocated to entanglement distribution between communicating parties. It is to be noted that, if the amount of EPR pair is less than the total length of the message block then EPR pairs are consumed

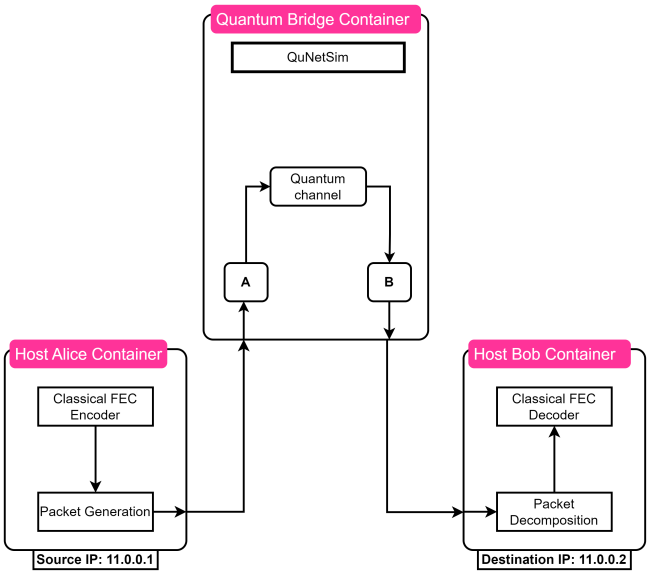

Fig. 4. Packet flow through various docker containers in ComNetsEmu.

first to carry out superdense coding; if there is still data to be sent, then remaining message is sent as one classical bit per qubit. To enforce superdense coding scheme, it is made sure that the amount of EPR pairs shared among Alice and Bob is exactly half of the size of the net message frame generated by Alice. Although intuitively one can extrapolate that, in the scenario when superdense coding is not used, the channel usage increases which can further affect the BER performance of the ECC.

The IP packet containing the message was encoded in various coding rates as depicted in Fig.5. The coding rate is a dynamic parameter and can be chosen arbitrarily or in response to the channel behavior. In this case, a rather small encoding scheme has been observed considering an IoT-based scenario where long codewords are typically avoided for stringent latency factor. Fig. 5 displays the trend of BER against increasing depolarizing probability p. For each data point plotted in Fig.5, 1000 iteration of transmission and reception of data packet was carried out. Due to long simulation time and limited CPU resource, the collection of data plotted is sparse. It is evident from the figure that the RS-coded packets experienced clear advantage in comparison to uncoded packets. RS$(40, 20)$ possessing higher redundancy at the cost of lower code rate have performed better in comparison to other coding rates. Until depolarising probability of 0.15, there is significant difference in terms of performance between the described coding rates; which further on reaches an intersection point as the noise increases. RS code displays reasonable performance signifying the potential usage of classical error correction schemes for CQ communication instead of using QEC which is highly complex and expensive.

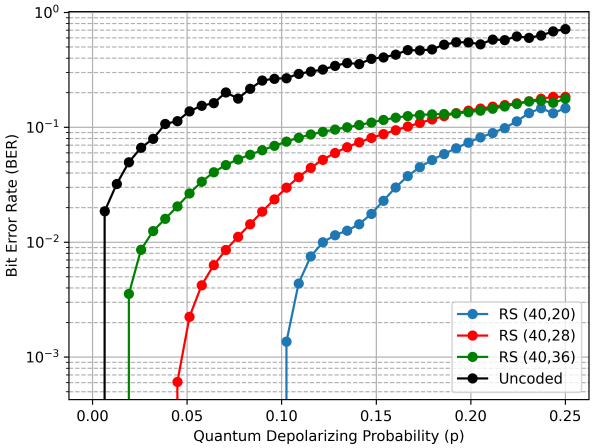

Fig. 5. BER plot against quantum depolarising probability (p) for RS code.

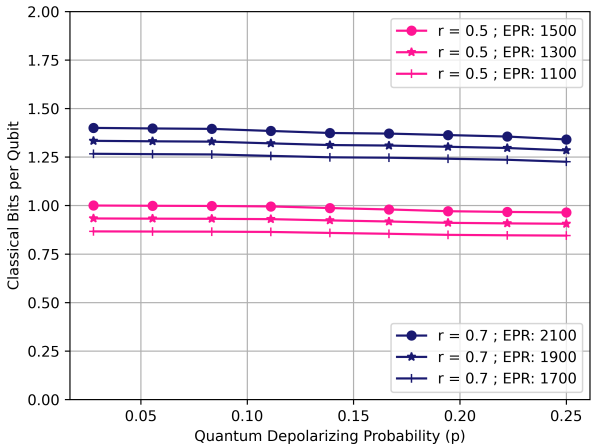

Fig. 6. Classical bit sent per qubit via depolarising channel.

The performance of RS code can be further enhanced by introducing puncturing or interleaving. Possible usage of other classical coding schemes such as Turbo codes, LDPC codes or polar codes can potentially produce better performance, for their capacity reaching capabilities.

B. Classical Bit per Qubit

In this section, we have analyzed the average amount of meaningful classical bits sent per qubit transmission $\mathcal{C}_{avg}$ in the noisy set up of depolarizing channel. In order to calculate the values of $\mathcal{C}_{avg}$, we have taken in account the net bit flips experienced due to the effect of the channel, coding rate of the FEC scheme, the amount of EPR pairs used, and the net amount of bits transferred per communication iteration. The detrimental effects of depolarizing channel on $\mathcal{C}_{avg}$ is plotted in Fig. 6. Three scenarios have been considered in observing the behavior of $\mathcal{C}_{avg}$ against noise. 1) Data transmission under normal condition where EPR pairs are not utilized, 2) data transmission utilizing superdense coding only, and 3) data transmission split between a portion utilising superdense coding and transmission of remaining bits one qubit per classical bit. If P is the number of packet, N is the total number of bits in the packet, E is the total EPR frames sent, L is the total number of EPR pairs in a frame, $\mathcal{E}$ is the number of erroneous bits, and r is the coding rate then for $EL = 0$ (one classical bit per qubit), $\mathcal{C}_{avg} = r - \mathcal{E}/(PN)$; when $EL \geq PN/2$ (superdense coding), $\mathcal{C}_{avg} = 2r - \mathcal{E}/(PN)$; and for $0 \leq EL \leq PN/2$ (a portion utilizing superdense coding and the rest allocating one qubit per classical bit),

$$\mathcal{C}_{avg} = \left(2r - \frac{\mathcal{E}}{PN} \times \frac{2EL}{PN}\right)\frac{2EL}{PN} + \left(r - \frac{\mathcal{E}}{PN} \times \left(1 - \frac{2EL}{PN}\right)\right)\left(1 - \frac{2EL}{PN}\right). \quad (7)$$

Here, the choice of coding rates have been kept uniform to previous simulation although the formula have been generalised for any FEC scheme. A sum of 3000 and 4200 bits have been sent for each data point for different coding rate scenarios along with varying net EPR pairs sent in between bursts. The points are experimental values, whereas the connecting lines are analytical. The trend in Fig. 6 signifies the classical bit(s) per qubit sent approaches values closer to the theoretical capacity of 2 while using the entanglement-assisted protocol of superdense coding. When the total amount of EPR pairs as a resource is less between the communicating parties, the net capacity falls. Higher coding rates enhances the capacity as it uses the channel more efficiently albeit at the cost of encountering more errors. Despite the fact that superdense coding scheme should ideally provide a capacity of 2, the inclusion of parameters (coding rate, channel error, and entanglement) in capacity calculation presents a rather practical trend.

C. Proof of Concept: Transmission of Mario Image

As a proof of concept, we have sent an image of Mario as depicted in Fig. 7 from Alice to Bob container. There are four color palettes in the image which can distinctly represent four different Bell states, hence four different permutation of two bits of classical information. Mario image was sent with and without encoding for comparison. The encoded images are show in Fig. 7 (d) and 7 (e), respectively. It has been encoded into RS$(10, 7)$ and RS$(13, 7)$ for comparison. Visually, it is clear that the uncoded image file is highly susceptible to errors whereas the RS coded Mario image was still able to withstand an error probability of $p = 0.2$ with distinguishable features.

V. Conclusion

We demonstrated a classical-quantum (CQ) network on the Qontainernet platform by transmitting classical packets through the integrated physical and link layers. The focus

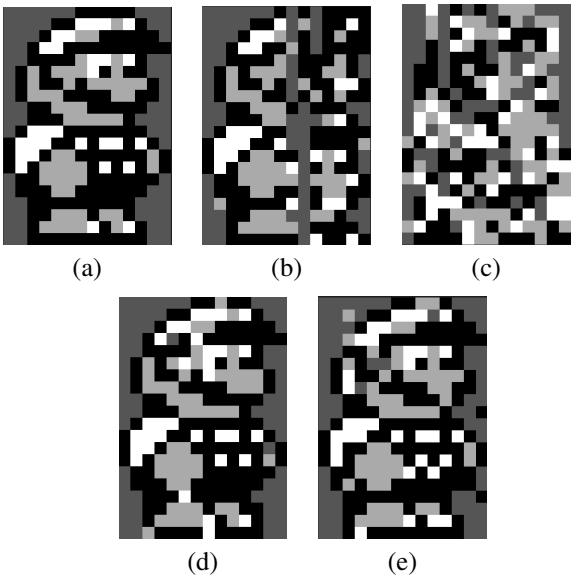

Fig. 7. Mario image through various cases of depolarising probability p. (a) Initial Mario image (b) Mario image with $p = 0.1$ (c) Mario image with $p = 0.2$ (d) Mario image with $p = 0.1$ and RS$(10, 7)$ (e) Mario image with $p = 0.2$ and RS$(13, 7)$

was on maintaining the existing classical architecture while efficiently incorporating quantum features in a straightforward manner. Analysis of the simulation-emulation process revealed an increase in capacity when sending classical messages over a quantum link using an entanglement-assisted communication protocol, consistent with the findings in [20]. The integration of simple classical error correction, specifically Reed-Solomon (RS) codes, for mitigating quantum errors showed promising results. This approach can be further enhanced with capacity-approaching error correction schemes such as Low-Density Parity-Check (LDPC) or Polar codes. For future work, we plan to explore the inclusion of other capacity-approaching classical error correction schemes. Given that IoT interconnects billions of devices, ensuring security for each link is critically important. The entanglement-assisted protocol implemented in this work could be extended to detect various adversarial attacks. However, the current emulation platform was slower due to the quantum integration, as QuNetSim is written in Python. To improve emulation speed, translating the implementation to lower-level languages like C or C^{++} will be considered. Finally, the point-to-point protocols will be scaled to support multiple users (N users) to fully realize the envisioned CQ internet model.

ACKNOWLEDGMENT

The authors would like to thank Leonardo Gonzalez for his advice on the simulation and analysis. This work has been partially funded by the German Research Foundation (DFG, Deutsche Forschungsgemeinschaft) as part of Germany's Excellence Strategy – EXC2050/1 – Project ID 390696704 – Cluster of Excellence "Centre for Tactile Internet with Human-in-the-Loop" (CeTI) of Technische Universität Dresden. The authors also acknowledge the financial support by the Federal Ministry of Education and Research of Germany in the programme of "Souverän. Digital. Vernetzt.". Joint project 6G-life, project identification number: 16KISK001K.

REFERENCES

[1] Cisco, "Internet of things," 2016.
[2] M. Giordani, M. Polese, M. Mezzavilla, S. Rangan, and M. Zorzi, "Toward 6g networks: Use cases and technologies," *IEEE Communications Magazine*, vol. 58, no. 3, pp. 55–61, 2020.
[3] M. Z. Chowdhury, M. Shahjalal, S. Ahmed, and Y. M. Jang, "6g wireless communication systems: Applications, requirements, technologies, challenges, and research directions," *IEEE Open Journal of the Communications Society*, vol. 1, pp. 957–975, 2020.
[4] D. C. Nguyen, M. Ding, P. N. Pathirana, A. Seneviratne, J. Li, D. Niyato, O. Dobre, and H. V. Poor, "6g internet of things: A comprehensive survey," *IEEE Internet of Things Journal*, vol. 9, no. 1, pp. 359–383, 2022.
[5] T. Q. Duong, J. A. Ansere, B. Narottama, V. Sharma, O. A. Dobre, and H. Shin, "Quantum-inspired machine learning for 6g: fundamentals, security, resource allocations, challenges, and future research directions," *IEEE Open Journal of Vehicular Technology*, vol. 3, pp. 375–387, 2022.
[6] G. Moore, "Moore's law," *Electronics Magazine*, vol. 38, no. 8, p. 114, 1965.
[7] P. Botsinis, D. Alanis, S. Feng, Z. Babar, H. V. Nguyen, D. Chandra, S. X. Ng, R. Zhang, and L. Hanzo, "Quantum-assisted indoor localization for uplink mm-wave and downlink visible light communication systems," *IEEE Access*, vol. 5, pp. 23327–23351, 2017.
[8] P. Botsinis, D. Alanis, Z. Babar, S. X. Ng, and L. Hanzo, "Joint quantum-assisted channel estimation and data detection," *IEEE Access*, vol. 4, pp. 7658–7681, 2016.
[9] P. Botsinis, D. Alanis, Z. Babar, H. V. Nguyen, D. Chandra, S. X. Ng, and L. Hanzo, "Quantum-aided multi-user transmission in non-orthogonal multiple access systems," *IEEE Access*, vol. 4, pp. 7402–7424, 2016.
[10] S. DiAdamo, J. Nötzel, S. Sekavčnik, R. Bassoli, R. Ferrara, C. Deppe, F. H. Fitzek, and H. Boche, "Integrating quantum simulation for quantum-enhanced classical network emulation," *IEEE Communications Letters*, vol. 25, no. 12, pp. 3922–3926, 2021.
[11] A. Pirker and W. Dür, "A quantum network stack and protocols for reliable entanglement-based networks," *New Journal of Physics*, vol. 21, no. 3, p. 033003, 2019.
[12] A. Dahlberg, M. Skrzypczyk, T. Coopmans, L. Wubben, F. Rozpedek, M. Pompili, A. Stolk, P. Pawełczak, R. Knegjens, J. de Oliveira Filho, *et al.*, "A link layer protocol for quantum networks," in *Proceedings of the ACM Special Interest Group on Data Communication*, pp. 159–173, 2019.
[13] Z. Shadman, H. Kampermann, D. Bruß, and C. Macchiavello, "Optimal superdense coding over memory channels," *Physical Review A*, vol. 84, no. 4, p. 042309, 2011.
[14] H. Zimmermann, "Osi reference model - the iso model of architecture for open systems interconnection," *IEEE Transactions on Communications*, vol. 28, no. 4, pp. 425–432, 1980.
[15] H. J. Briegel, W. Dür, J. I. Cirac, and P. Zoller, "Quantum repeaters for communication," 1998.
[16] N. Yu, C.-Y. Lai, and L. Zhou, "Protocols for packet quantum network intercommunication," *IEEE Transactions on Quantum Engineering*, vol. 2, p. 1–9, 2021.
[17] R. Cleve, D. Gottesman, and H.-K. Lo, "How to share a quantum secret," *Physical Review Letters*, vol. 83, p. 648–651, 7 1999.
[18] S. Das, R. Bassoli, R. Ferrara, J. Noetzel, C. Deppe, F. H. P. Fitzek, and H. Boche, "Comparative study of quantum and classical error correction for future quantum-6g networks," in *European Wireless 2022; 27th European Wireless Conference*, pp. 1–6, 2022.
[19] C. E. Boyd, "Classical error-correcting codes in quantum communications," 2014.
[20] J. Nötzel and S. DiAdamo, "Entanglement-assisted data transmission as an enabling technology: A link-layer perspective," in *2020 IEEE International Symposium on Information Theory (ISIT)*, pp. 1955–1960, 2020.